Photoinduced magnetization enhancement in two-dimensional weakly anisotropic Heisenberg magnets

Caretta, Antonio; Donker, Michiel C.; Polyakov, Alexey O.; Palstra, Thomas T. M.; van Loosdrecht, Paul H. M.

Published in:
Physical Review. B: Condensed Matter and Materials Physics

DOI:
10.1103/PhysRevB.91.020405

Publication date:
2015

PHYSICAL REVIEW B **91**, 020405(R) (2015)

Photoinduced magnetization enhancement in two-dimensional weakly anisotropic Heisenberg magnets

Antonio Caretta,* Michiel C. Donker, Alexey O. Polyakov, Thomas T. M. Palstra, and Paul H. M. van Loosdrecht†
Zernike Institute for Advanced Materials, University of Groningen, Nijenborgh 4, 9747 AG Groningen, The Netherlands
(Received 10 March 2014; revised manuscript received 11 December 2014; published 20 January 2015)

By comparing the photoinduced magnetization dynamics in simple layered systems we show how light-induced modifications of the magnetic anisotropy directly enhance the magnetization. It is observed that the spin precession in $(CH_3NH_3)_2CuCl_4$, initiated by a light pulse, increases in amplitude at the critical temperature T_C. The phenomenon is related to the dependence of the critical temperature on the axial magnetic anisotropy. The present results underline the possibility and the importance of the optical modifications of the anisotropy, opening different paths toward the control of the magnetization state for ultrafast memories.

DOI: 10.1103/PhysRevB.91.020405 PACS number(s): 78.20.Ls, 75.30.Gw, 76.50.+g, 78.67.Pt

Fast and efficient control of the magnetic state of a material requires the understanding of nonequilibrium processes occurring in the picosecond time regime. The importance of studying the magnetic phenomena with femtosecond time resolution was first demonstrated by Beaurepaire *et al.* [1]. In this work it was found that ferromagnetic Ni could be demagnetized with ultrashort optical pulses within 1 ps. Shortly after this observation, a number of experiments showing optical manipulation of the magnetization were published [2–4]. The photogeneration of coherent spin precession as well as the possibility of controlling the spin precession direction via the inverse Faraday effect [5] were demonstrated. These investigations led finally to the spectacular observation of all-optical magnetization switching in GdFeCo [6]. Recently, the field of ultrafast magnetization, "femtomagnetism" [7], started to address increasing attention towards other possible ultrafast switches: propagating acoustic phonons [8,9] and spin waves [10], or spin polarized electron transport [11] and spin transfer torque [12]. All these phenomena are essentially nonequilibrium processes, and the ability to control the magnetic state of a material by optical pulses has obvious potential in applications. The generation of coherent spin precession is a possible method to control the magnetic state of a system.

A spin precession can be initiated by an optical pulse via different mechanisms. Ultrafast demagnetization in metallic thin films can, for instance, induce a fast (<10 ps) spin reorientation [3,13]. Also, the use of circularly polarized optical pulses can efficiently initiate a precession [5,14]. The first method relies on fast demagnetization rates, and the second on the transparency of the material and strong spin-orbit coupling. In order to investigate other mechanisms of spin reorientation, we measured two insulating magnetic materials, characterized by a unique range of parameters, a low demagnetization rate, and nearly quenched spin-orbit coupling. The organic-inorganic hybrid materials realize these requirements, since they are structurally versatile and tunable [15,16]. In particular, it would be interesting to investigate the effect of nonequilibrium modifications of the magnetic parameters such as single-ion magnetic anisotropy. The modifications of the magnetic anisotropy show up, phenomenologically, at time scales only limited by the magnetic response of the system, the spin precession period. These processes might be extremely relevant for understanding all-optical magnetization control, but few experiments address this issue.

In this Rapid Communication we report on optical time-resolved Faraday rotation (FR) experiments on simple magnetic systems, the layered organic-inorganic hybrids (OIHs). The magnetic field and temperature dependence of the light-induced precession are studied in two model systems: ferromagnetic $(CH_3NH_3)_2CuCl_4$ (MACuCl), and antiferromagnetic $(CH_3CH_2NH_3)_2CuCl_4$ (EACuCl). The observed difference in response of the two materials strongly suggests that, even in the low-fluence regime, the magnetization enhancement of the spin precession observed in MACuCl is due to a nonequilibrium increase of the axial magnetic anisotropy.

The layered Cu-based organic-inorganic hybrids studied here are nearly ideal two-dimensional Heisenberg ferromagnets and have been widely studied in the 1970's [17]. The structure is constituted by corner sharing $CuCl_6$ octahedra, forming the inorganic layers, and bilayers of organic cations, attached to the octahedra by NH_3 heads [18,19] [Fig. 1(b)]. The proper Hamiltonian to describe the single layer magnetism is [17]

$$\mathcal{H} = -2J \sum_{i>j} \vec{S}_i \cdot \vec{S}_j + \sum_i \left(K S_{yi}^2 + D S_{zi}^2 \right), \qquad (1)$$

where $\vec{S}_i$ is the spin of the ith site, S_{yi} and S_{zi} are respectively the y and z components of the spin, and $K > 0$ and $D > 0$ express the magnetic anisotropy. The intralayer exchange J is ferromagnetic due to cooperative Jahn-Teller ordering [20], with $J/k_B \sim 20$ K. The exchange interaction between the layers is expressed with J' [Fig. 1(b)], and the Hamiltonian is modified by an additional term accounting for the other layers (see Ref. [21]). The interlayer exchange J' is up to five orders of magnitude smaller than J, and determines the overall three-dimensional magnetic character of the compound: While MACuCl orders ferromagnetically at 8.9 K, EACuCl orders antiferromagnetically at 10.2 K [17]. It is well known that two-dimensional (2D) Heisenberg magnets do not order at any finite temperature [22]. The only possible cause of ordering in

*antonio.caretta@elettra.eu
†pvl@ph2.uni-koeln.de

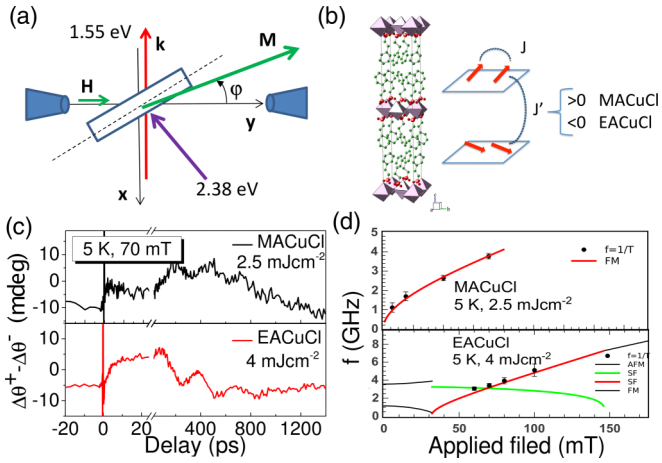

FIG. 1. (Color online) (a) Experiment scheme. (b) Crystal structure of EACuCl and summary of exchange constants. (c) Magnetization dynamics in MACuCl and EACuCl at 70 mT and 5 K. (d) Precession frequency measured from the Faraday rotation in MACuCl (up) and EACuCl (down). The $f(H)$ curves represent the resonance frequency in the antiferromagnetic (AFM), the spin-flip (SF), and the ferromagnetic (FM) phases (EACuCl: More details can be found in Ref. [34]).

Cu-based OIHs is the presence of finite interlayer exchange J', breaking the 2D character, or axial magnetic anisotropy $H_A^{\text{Ising}} \equiv 2KS/g\mu_B$ [23]. The preferential axis breaks the continuous symmetry and the system behaves similarly to an Ising 2D magnet, thus ordering at a finite temperature [24–26]. The largest of the deviations from the ideal situation causes magnetic ordering. In Table I the magnetic parameters describing MACuCl and EACuCl are shown, with the use of the intralayer effective field $H_E = 2zJS/g\mu_B$ (z is the number of neighbors in the layer). Specifically, for MACuCl, $H_A^{\text{Ising}}/H_E > |J'/J|$. Vice versa for EACuCl, $H_A^{\text{Ising}}/H_E < |J'/J|$ (see Table I). It is very important to recall the dependence of the critical temperature T_C on the magnetic anisotropy, when $H_A^{\text{Ising}}/H_E > |J'/J|$ [24–26]:

$$T_C = \frac{4\pi J}{\ln(J/K)}. \tag{2}$$

It is clear that modifications of K, thus H_A^{Ising}, will only affect MACuCl, as instead in EACuCl the critical temperature is, in first approximation, only a function of J' [21].

TABLE I. Parameters characterizing the magnetic phases of MACuCl and EACuCl [17,27]: the critical temperature T_C, the intralayer ferromagnetic exchange $J/k \sim 20$ K, and the interlayer exchange J'. The planar and the axial anisotropy effective fields, respectively $H_A^{XY} \equiv 2DS/g\mu_B$ and $H_A^{\text{Ising}} \equiv 2KS/g\mu_B$, are normalized by the intralayer effective field $H_E = 2zJS/g\mu_B$, where $z = 4$ is the number of neighbors in the layer.

	T_C (K)	J/k_B (K)	J'/J	H_A^{Ising}/H_E	H_A^{XY}/H_E
MACuCl	8.9	19.2	$+5.5 \times 10^{-5}$	1.6×10^{-4}	3×10^{-3}
EACuCl	10.2	18.6	-8×10^{-4}	1.6×10^{-4}	3×10^{-3}

The samples are grown from solution in analogy to $(C_6H_5CH_2CH_2NH_3)_2CuCl_4$ (PEACuCl) (see Refs. [18,28]). The sample thickness is approximately 150 μm. Magnetic properties are probed by Faraday rotation, at a fixed frequency of 1.55 eV (800 nm). Time-resolved experiments are performed using a 1 kHz Ti:sapphire based amplified laser system (Hurricane, Spectra-Physics). The 2.38 eV (520 nm) pump is generated using a nonlinear optical parametric amplifier (Light Conversion). The 520 nm pulses are optimally tuned to the Cu-Cl charge transfer edge [29,30]. The pump fluence used in the experiments ranges from 2.5 to 4 mJ cm^{-2}, corresponding to a temperature increase of approximately 1 K (see the Supplemental Material [31]). The time resolution of the experiment is approximately 150 fs [32]. Magnetic measurements are performed in tilted-Voigt geometry, with an applied magnetic field along $\hat{y}$ perpendicular to the light propagation along $\hat{x}$ [Fig. 1(a)]. The linearly polarized pump electric field is oriented along $\hat{z}$, parallel to the crystal optical axis. The samples are rotated $\varphi_0 \sim 45^\circ$ around the $\hat{z}$ axis. In this configuration the FR is expressed by

$$\theta \propto \vec{k} \cdot \vec{M} \propto |M| \sin(\varphi), \tag{3}$$

where φ is the angle between the magnetization $\vec{M}$ and $\hat{y}$. The experimental data are represented as $(\Delta\theta^+ - \Delta\theta^-)$, where $\Delta\theta^+$ is the FR signal measured at positive applied field $+H$ and $\Delta\theta^-$ at $-H$. It is easy to note that (see the Supplemental Material [31])

$$\Delta\theta^+ - \Delta\theta^- \propto \left(\frac{\Delta M}{M_0} + m(T)\Delta\varphi\right), \tag{4}$$

where M_0 is the saturated magnetization measured at 0 K, ΔM and $\Delta\varphi$ are the pump-induced changes in magnetization and orientation, and $m(T) \equiv M(T)/M_0$ is the normalized magnetization [33]. It is important to note that at low temperatures, where $m(T) \sim 1$, we are sensitive to changes in φ while close to T_C, where $m(T) \sim 0$, modification of the magnetization absolute value dominates. Because of this, at high temperatures, variations in the magnetization orientation should be enormous to compensate for the low value of $m(T)$.

The magnetization dynamics, in both MACuCl and EACuCl, is characterized by two time regimes. The time dependence of the Faraday rotation at 70 mT and 5 K, in MACuCl and EACuCl, respectively, is shown in Fig. 1(c). At early time scales, up to 20 ps after the pump arrival, the magnetization increases by approximately 0.5%–1% with a rise time $\tau < 10$ ps (see the Supplemental Material [31]). This increase does not depend on the applied field or on the pump polarization. Later times are instead characterized by oscillations having an amplitude of the same order as the initial increase and a period strongly dependent on the applied magnetic field. The oscillation frequency $f = 1/T$ of MACuCl and EACuCl [top and bottom of Fig. 1(d)] at 5 K is shown as a function of the applied field. The data points are compared with the expected magnetic resonance curves. For MACuCl, $f = \gamma \frac{g}{4\pi}\sqrt{H(H + H_A)}$ [3] is used, where γ is the gyromagnetic factor, g the Landau splitting factor, and $H_A \sim 200$ mT, consistent with the static anisotropy field H_A^{XY} reported in literature (see also Table I). For EACuCl the precession frequency matches the antiferromagnetic resonance

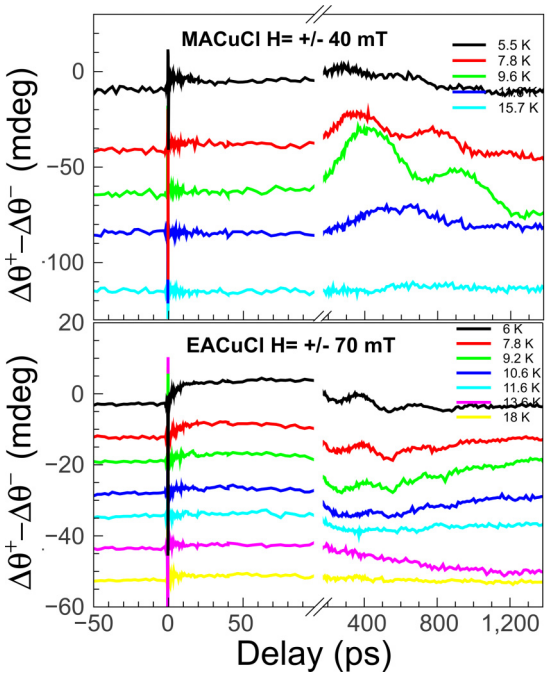

FIG. 2. (Color online) Temperature dependence of the magnetization dynamics in MACuCl (top, $H = \pm 40$ mT) and EACuCl (bottom, $H = \pm 70$ mT).

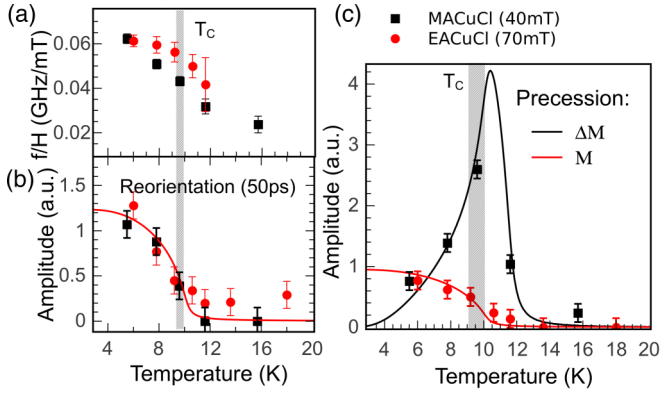

FIG. 3. (Color online) (a) Precession frequency (normalized by the applied field); (b) reorientation amplitude (at 50 ps delay) and (c) precession amplitude in MACuCl and EACuCl as a function of temperature. Note that the amplitudes are expressed as $(\Delta\theta^+ - \Delta\theta^-)/(\theta_0^+ - \theta_0^-)$. M and ΔM are respectively the magnetization and its derivative calculated at an applied field comparable to the experiment.

frequency reported in literature [34], as is shown in Fig. 1(d). The agreement between the photoinduced precession and the static magnetic resonance has two important implications: (i) The low temperature magnetic dynamics is dominated by precessional effects, and not by absolute value changes of M, and (ii) the initial increase in the magnetic signal is due to a initial rotation of the magnetization vector *toward* the inorganic planes. Such reorientation can be understood only by assuming an increase of either J or H_A.

While the low temperature magnetic field behavior of MACuCl and EACuCl is analogous, the response of the two systems is radically different when crossing the critical temperature. The temperature dependence of the magnetization dynamics in MACuCl (top) and EACuCl (bottom) is shown in Fig. 2. The measurements are performed at a fixed applied field. It can be easily observed that, while in EACuCl the magnetic signal simply disappears with increasing temperature, in MACuCl the precession amplitude grows to a maximum at 9.6 K, close to T_C. In both compounds the initial increase of the magnetization, between 10 and 100 ps, smoothly decreases with increasing temperature. Also the precession frequency, weakly decreasing at higher temperatures, seems to be comparable in the two materials. In order to quantify these observations, we estimate the initial reorientation amplitude by plotting the increase of $\Delta\theta^+ - \Delta\theta^-$ at 50 ps; the amplitude and the frequency of the precession are estimated from the oscillation maxima. Note that the precession frequencies are normalized by the external magnetic field H, as f/H. The resulting graphs are shown in Fig. 3, where MACuCl and EACuCl are compared. As expected, the behavior of the two compounds is analogous when looking at the normalized precession frequency f/H and the initial reorientation [Figs. 3(a) and 3(b)]. The initial reorientation scales as the spontaneous magnetization $m(T)$, thus sharply decreases as T_C is approached from below, supporting the observation that the initial dynamics is dominated by the reorientation of the magnetization, rather than a change in its absolute value [35]. The precession frequency shows a gentle redshift with increasing temperature, in line with a temperature dependence of the spin resonance. The most striking difference between MACuCl and EACuCl is the amplitude of the oscillation [Fig. 3(c)], which decreases to zero at T_C in the latter and grows by a factor of 3, when compared to the value at 4 K, in the former.

The enhancement of the magnetization absolute value observed in MACuCl, and peaked at T_C, can be explained by a nonequilibrium increase in the axial anisotropy. It is safe to assume that the pump pulses produce the same electronic and structural modifications in both compounds at short (50 ps) time scales since, in first approximation, both compounds can be considered as stacks of loosely coupled ferromagnetic layers. In fact, the layers in the two compounds are essentially the same (see Table I), thus the response to the optical excitation, at least within the layers, must be analogous in the two systems. As shown in Eq. (4), the FR signal is the sum of an angular term, proportional to the magnetization $m(T)$, and a term proportional the relative changes of the absolute magnetization M. Close to T_C, $m(T)\Delta\varphi \sim 0$, and the observed changes of FR are dominated by changes of the absolute magnetization M. Clearly, although the two systems initially behave similarly [Fig. 3(b)], the absolute magnetization of MACuCl increases in proximity to T_C at later times, as shown by the precession amplitude [Fig. 3(c)]. The Ising anisotropy is the only layer parameter which, in first approximation, can specifically affect the magnetization dynamics in MACuCl, leaving EACuCl unperturbed. In fact, assuming sizable changes of H_A^{Ising} [thus changes of K in Eq. (2)], only the critical temperature of MACuCl would have notable modifications. Changes in the critical temperature value are enhanced at T_C, where the slope of the spontaneous magnetization is larger. This is indeed observed in MACuCl,

and it is easy to quantify the effect. The relatively slow time scale (400 ps) at which the magnetization enhancement takes place also suggests that the phenomenon should be described in terms of quasiequilibrium dynamics.

The increase of magnetization in MACuCl, due to an increase of the anisotropy H_A^{Ising}, can be easily estimated from Eq. (2). The increase of T_C in MACuCl caused by an increase of the anisotropy $K + \Delta K$ is

$$T_C(K + \Delta K) = T_C \left(1 + \frac{1}{\ln(J/K)} \frac{\Delta K}{K}\right). \tag{5}$$

In the specific case of MACuCl we have

$$\Delta T_C \sim \frac{T_C}{10} \frac{\Delta K}{K} \sim \frac{\Delta K}{K}.$$

Additionally, the magnetization, because of an increase in T_C, is enhanced and the effect is larger in particular at the critical temperature, since

$$\frac{\Delta M}{M_0} = \left|\frac{\partial m}{\partial T}\right| \Delta T_C \sim \left|\frac{\partial m}{\partial T}\right| \frac{\Delta K}{K}.$$

In Fig. 3(c), $\Delta M \propto \frac{\partial m}{\partial T}$ is calculated from the magnetization curve M in the applied field (see the Supplemental Material [31]) and is respectively shown as black and red curves. Given that, close to T_C, $\frac{\Delta M}{M_0} \sim 0.03$ in MACuCl, and that the maximum of $\frac{\partial m}{\partial T}$ is approximately 0.4, we obtain an increase of the anisotropy of $\frac{\Delta K}{K} \sim 10\%$.

Such a small increase of the magnetic anisotropy, which perfectly describes the observations, does not influence the values of the precession frequencies measured at 5 K. In particular, it has no role in the magnetization dynamics in EACuCl, and the precession amplitude simply scales as the magnetization $m(T)$, reducing to zero at T_C, as indeed observed.

We now briefly discuss the origin of the anisotropy enhancement. First, we note that the time scales of the phenomenon, of approximately 400 ps, indicate that the origin of the process involves thermal effects, such as phonon or magnon propagation and thermalization. Additionally, the low-fluence excitation regime and the strong dielectric character of the hybrid materials suggest that typical electronic effects, such as magnetization or spin-orbit quenching, are not relevant in present conditions. A possible explanation is given in analogy to Ref. [9]. The essential idea is that the photogenerated acoustic phonons distort the lattice and, due to magnetoelastic coupling, the axial anisotropy is increased. In Ref. [9] uniaxial stress, generated at the interface of a specially designed layer structure, is applied to the magnetic layer. The optical excitation in the layered hybrids will not be isotropic because of the appreciable difference in linear absorption along the optical axes. Acoustic phonons are nearly instantaneously created by the pump pulses, and generate a long lasting (400 ps) anisotropic distortion, consistent with our FR experiments.

The effect of anisotropy-induced magnetization enhancement can be increased by using multilayer structures based on thin permalloy layers and dielectric spacers. Permalloy materials are well known for their high critical temperature and high magnetic permeability. These properties result from respectively a large magnetic exchange J and a low single ion anisotropy K. As a consequence, permalloy materials are good approximations of Heisenberg systems, with critical temperatures up to $T_C = J/k_B \sim 1000$ K. As was outlined before, when thin films are formed, the critical temperature is expected to decrease, because of the increasing two-dimensional character of the system [36]. For a thin enough system, Eq. (2) is applicable and the layer ordering temperature is largely reduced. By using, as an interlayer spacer, a material that can induce stress (e.g., piezoelectric) when an external stimulus is applied, the magnetization can be largely enhanced. For instance, one monolayer of $Ni_{83}Fe_{17}$ orders at approximately $T_C/3 \sim 850$ K$/3 \sim 283$ K [37]. Assuming a relative increase of the anisotropy of 10% ($\Delta K/K = 0.1$) and $J/K \sim 10^5$ as in the hybrids, an increase of the critical temperature of 8.5 K is predicted from Eq. (5). This device would work perfectly in the room temperature regime, where the critical temperature can be optimally tuned by the layer thickness. Additionally, the spacer can be selected as a function of different external stimuli, the only condition being a sufficient modification of the anisotropy K.

In conclusion, the magnetization dynamics in both MACuCl and EACuCl can be fully described by a photoinduced enhancement of the axial anisotropy, which causes an increase in the magnetization precession amplitude in MACuCl close to T_C. The mechanism described in this Rapid Communication is applicable also to multilayer structures consisting of a combination of piezoelectric layers and magnetic layers with a strain dependent anisotropy, and in this way we expect that one can even design devices that are functional at room temperature.

We acknowledge Professor Dr. A. V. Kimel, D. Bossini, and Dr. R. I. Tobey for useful discussions.

[1] E. Beaurepaire, J.-C. Merle, A. Daunois, and J.-Y. Bigot, Phys. Rev. Lett. **76**, 4250 (1996).

[2] G. Ju, A. V. Nurmikko, R. F. C. Farrow, R. F. Marks, M. J. Carey, and B. A. Gurney, Phys. Rev. Lett. **82**, 3705 (1999).

[3] M. van Kampen, C. Jozsa, J. T. Kohlhepp, P. LeClair, L. Lagae, W. J. M. de Jonge, and B. Koopmans, Phys. Rev. Lett. **88**, 227201 (2002).

[4] A. V. Kimel, A. Kirilyuk, A. Tsvetkov, R. V. Pisarev, and T. Rasing, Nature (London) **429**, 850 (2004).

[5] A. V. Kimel, A. Kirilyuk, P. A. Usachev, R. V. Pisarev, A. M. Balbashov, and T. Rasing, Nature (London) **435**, 655 (2005).

[6] C. D. Stanciu, F. Hansteen, A. V. Kimel, A. Kirilyuk, A. Tsukamoto, A. Itoh, and T. Rasing, Phys. Rev. Lett. **99**, 047601 (2007).

[7] A. Kirilyuk, A. V. Kimel, and T. Rasing, Rev. Mod. Phys. **82**, 2731 (2010).

[8] J.-W. Kim, M. Vomir, and J.-Y. Bigot, Phys. Rev. Lett. **109**, 166601 (2012).

[9] O. Kovalenko, T. Pezeril, and V. V. Temnov, Phys. Rev. Lett. **110**, 266602 (2013).
[10] T. Satoh, Y. Terui, R. Moriya, B. A. Ivanov, K. Ando, E. Saitoh, T. Shimura, and K. Kuroda, Nat. Photon. **6**, 662 (2012).
[11] A. Eschenlohr, M. Battiato, P. Maldonado, N. Pontius, T. Kachel, K. Holldack, R. Mitzner, A. Fölisch, P. M. Oppeneer, and C. Stamm, Nat. Mater. **12**, 332 (2013).
[12] P. Nemec, E. Rozkotova, N. Tesarova, F. Trojanek, E. De Ranieri, K. Olejnik, J. Zemen, V. Novak, M. Cukr, P. Maly, and T. Jungwirth, Nat. Phys. **8**, 411 (2012).
[13] The change in the shape anisotropy is the nonequilibrium condition for precession: The reorientation of the equilibrium axis is as fast as the demagnetization in the material.
[14] D. Bossini, A. M. Kalashnikova, R. V. Pisarev, T. Rasing, and A. V. Kimel, Phys. Rev. B **89**, 060405 (2014).
[15] D. B. Mitzi, Prog. Inorg. Chem. **48**, 1 (1999).
[16] C. N. R. Rao, A. K. Cheetham, and A. Thirumurugan, J. Phys.: Condens. Matter **20**, 083202 (2008).
[17] L. J. de Jongh and A. R. Miedema, Adv. Phys. **23**, 1 (1974).
[18] A. O. Polyakov, A. H. Arkenbout, J. Baas, G. R. Blake, A. Meetsma, A. Caretta, P. H. M. van Loosdrecht, and T. T. M. Palstra, Chem. Mater. **24**, 133 (2012).
[19] A. Caretta, R. Miranti, R. W. A. Havenith, E. Rampi, M. C. Donker, G. R. Blake, M. Montagnese, A. O. Polyakov, R. Broer, T. T. M. Palstra, and P. H. M. van Loosdrecht, Phys. Rev. B **89**, 024301 (2014).
[20] D. Khomskii and K. Kugel, Solid State Commun. **13**, 763 (1973).
[21] L. J. de Jongh and H. E. Stanley, Phys. Rev. Lett. **36**, 817 (1976).
[22] N. D. Mermin and H. Wagner, Phys. Rev. Lett. **17**, 1133 (1966).
[23] For $D \gg K$ the layer has planar anisotropy, and for $D \simeq K$ axial anisotropy. The magnetic system can be described respectively with an XY model or a Ising model, thus the names H_A^{XY} and H_A^{Ising}.
[24] M. Bander and D. L. Mills, Phys. Rev. B **38**, 12015 (1988).
[25] R. P. Erickson and D. L. Mills, Phys. Rev. B **43**, 11527 (1991).
[26] E. Kuz'min and G. Petrakovskii, Sov. Phys. J. **31**, 256 (1988).
[27] A. H. Arkenbout, Ph.D. thesis, University of Groningen, The Netherlands, 2010.
[28] H. Arend and W. Huber, J. Cryst. Growth **43**, 213 (1978).
[29] G. Heygster and W. Kleemann, Physica B & C **89**, 165 (1977).
[30] A. Caretta, R. Miranti, A. H. Arkenbout, A. O. Polyakov, A. Meetsma, R. Hidayat, M. O. Tjia, T. T. M. Palstra, and P. H. M. v. Loosdrecht, J. Phys.: Condens. Matter **25**, 505901 (2013).
[31] See Supplemental Material at http://link.aps.org/supplemental/10.1103/PhysRevB.91.020405 for a detailed description of the experimental set-up, the magnetic field dependence of the Faraday rotation and the short time-scale magnetization dynamics.
[32] The cross correlation had been measured on a ZnSe nonlinear crystal and on the sample itself.
[33] $m(T)$ is the magnetization calculated in the presence of a small magnetic field, as in the experiments.
[34] M. Tanimoto, T. Kato, and Y. Yokozawa, Phys. Lett. A **58**, 66 (1976).
[35] In fact, as given in Eq. (4), the angular term $\Delta\varphi$ is scaled by $m(T)$ [red curve in Fig. 3(b)].
[36] F. Huang, M. T. Kief, G. J. Mankey, and R. F. Willis, Phys. Rev. B **49**, 3962 (1994).
[37] J. Dubowik, F. Stobiecki, and T. Luciński, Phys. Rev. B **57**, 5955 (1998).